Using seismic guided EM inversion to explore a complex geological area: An application to the Kraken and Bressay heavy oil discoveries, North Sea

Zhijun Du, PGS*

Summary

The integrated analysis of controlled source electromagnetic (CSEM) with seismic data can provide valuable information on reservoir characteristics. We introduce in this paper a method for integrating Towed Streamer EM and dual-sensor seismic data and refer to it as seismic guided EM inversion. The inversion workflow is initiated by adopting a sparse-layer depth model defined by the dual-sensor seismic data to suggest resistivity boundaries without a rigid constraint. This makes good sense when considering the uncertainties in the seismic data from the time to depth conversion, and more importantly, the fact that a reservoir can be hydrocarbon-charged to an unknown degree corresponding to the spill-point or less. The anisotropic resistivity variations within the layers are accommodated by the lower and upper boundaries, which can be estimated by the unconstrained 2.5D anisotropic inversions. To demonstrate the workflow, we apply it to a dataset acquired in an area with complex geology resulting in challenging imaging issues of the Kraken and Bressay fields. The two heavy oil reservoirs are rich in injectites, located in close proximity to other high resistivity settings, such as the shallow gas pockets in the overburden, the regional Balder Tuff and a few granite intrusions.

Introduction

The ideal companion to high quality marine CSEM data is 3D seismic data, and the application of joint interpretation of seismic and marine CSEM in de-risking exploration prospects has led to a significant number of success stories since 2000 (e.g. Karman, et al., 2013). When assessing the prospectivity in complex geological regions, where seismic provides a high resolution structural image of the subsurface, marine EM estimates the resistivity of assumed reservoirs, and as such is more sensitive to the presence of hydrocarbons. The integration of seismic with CSEM data can thus provide subsurface information that is either unreliable or simply unavailable when only a single data type is used.

While several methods for joint interpretation of multiple geophysical data exist, we discuss here a possible way to make the inversion-based EM and seismic integration process more data and information-driven and less *a priori* model driven. The methods that involve the use of structural properties, i.e. boundaries of geological targets, where the EM inversion is regularized by the structural information from the higher resolution of the seismic imaging (e.g., Morten et al. 2013). The workflow for conducting such constrained EM inversions is generally initialized by dividing the background resistivity model into large volumes of homogeneous regions. The regularization process requires reliable *a priori* resistivity information to populate the seismically defined volumes. However, this is only possible if the study area displays homogeneous stratigraphy, in other situations, i. e., existence of lateral strata variation and anisotropy, it is difficult or impossible to build the required *a priori* model from limited available information. In this paper, we introduce and test a different approach for integrating Towed EM and dual-sensor seismic data. Our approach is based on the concept of 'guidance'. The workflow is initiated by adopting a sparse-layer depth model defined by high resolution seismic to suggest resistivity boundaries for the EM inversion without a rigid constraint, whereas the resistivity variations within the layers are set by plausible lower and upper boundaries. We show the workflow for integrating the towed streamer EM and dual-sensor seismic data by applying the method to an area with complex geology and challenging imaging issues of the Kraken and Bressay fields.

The BBK region and Towed EM data

In 2012 PGS conducted a towed streamer EM survey over Bressay, Bentley and Kraken (BBK) heavy oil fields in the North Sea using the newly developed controlled-source Towed Streamer EM acquisition system (Figure 1). The BBK discoveries were considered to pose several challenges to conventional CSEM surveying. The very shallow depth of water, 90 - 130 m, dampen the EM anomalies due to airwave coupling. The formation within the block consists of coarse clastics, which lead to the further formation of a prograding delta compound. The reservoirs are to a large extent injectites, located in close depth proximity to other high resistivity settings, such as the regional Balder Tuff, and granite intrusions. The geology in the region is thus complex resulting in challenging imaging issues. The heavy oil charge means there is no direct hydrocarbon indication in the seismic data, due to the low acoustic impedance contrast between the reservoir and its surrounding shale.

The Towed EM system for the BBK survey consisted of a ~7.7 km receiver cable deployed at 50 -100 m water depth, and a powerful (1,500 A) 800 m long bipole source towed at 10 m depth. Using a 4-knot towing speed, the acquisition pattern was based on a source signal every 250 m and 44 unique receiver positions for each "shot". Compared to a conventional node-based marine controlled-source

DOI http://dx.doi.org/10.1190/segam2014-0534.1

electromagnetic (CSEM) system, where the receivers are very sparsely placed on the seafloor in a line or areal pattern, approximately 1 km apart, the highly sensitive receiver electrodes housed in the streamer of the towed EM system are able to densely sample the subsurface with an average offset interval of ~160 m over offset ranges of ~800 to 7595 m. The Towed Streamer EM system thus provides the dense sampling, data quality and signal-to-noise ratio required for imaging challenging targets in a shallow water environment.

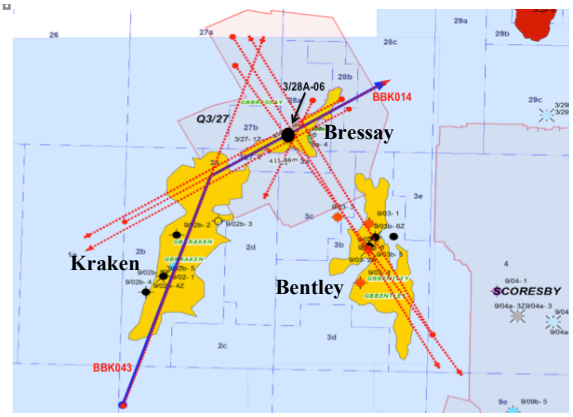

Figure 1: The Towed Streamer EM BBK survey area, where the red lines indicate the towed streamer EM lines. The well log, 3/28A-06, is located approximately at the central of Bressay, as indicated by the big black dot.

The unconstrained inversion

The final processed BBK towed streamer EM data set consists of six discrete transmission frequencies (0.2, 0.4, 0.6, 0.8, 1, 1.2 Hz). The dataset was inverted using the MARE2DEM codes, which is an Occam based 2.5D inversion build around a parallel adaptive finite element algorithm (Key, 2012). We parameterized the model domain with a dense grid of around 15,000-20,000 unknown resistivity parameters (depending on the profile length) from the seafloor to a depth of 2 km. We set a 1% error floor to the data and found that most of the survey profiles could be fit to a root-mean-squared (RMS) misfit of about 1.0 to 1.5 percent within 10-15 Occam iterations.

The unconstrained blind (without considering field geology) inversion for anisotropic resistivities started from an isotropic 1.0 Ωm half space. Figure 2 shows the inversion results (vertical resistivities only, and horizontal resistivities are not shown for brevity) from two towed streamer EM lines: BK043 and BK014 (Figure 1). The unconstrained inversion seeks the best model to fit the data that is also the smoothest model in the first derivative sense (Constable et al., 1987). Although the unconstrained inversion takes no account of complex or higher dimensional structures, it allows the class of structures to which the data are most sensitive, and variations in these structures to be assessed. By overlaying the retrieved resistivity model on the top of the coincident 2D seismic sections, the co-rendered images confirm the inversions have recovered the resistive basements. It has also revealed several large localized significant increases in resistivity between depth range of 0 - 1km (Figure 2).

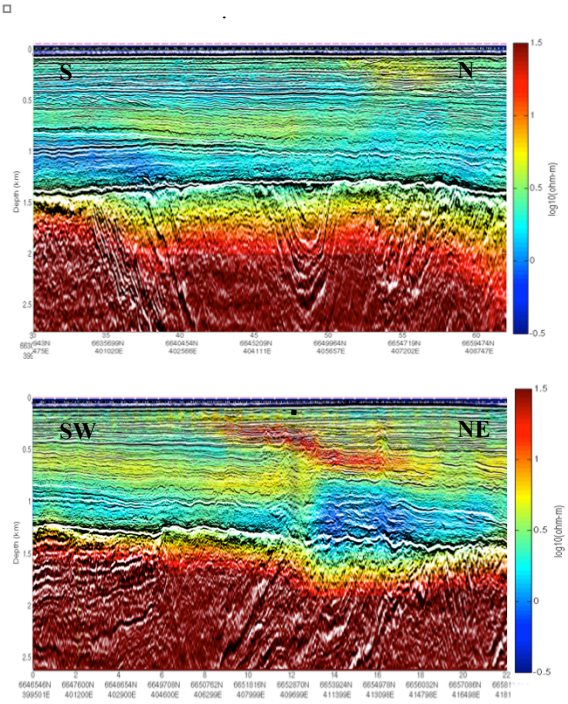

Figure 2: The results of the 2.5D unconstrained anisotropic inversion. The vertical resistivities are co-rendered with the coincident depth converted seismic sections. Top, for line BK043, and bottom, for line BK014. The black dotted line indicates the location of the Bressay 3/28A-6 well.

We calibrate the resistivity model recovered from the inversion of towed streamer EM line BK014 with the Bressay well-log, 3/28A-06, located close to the middle of the reservoir (Figure 2). The result of the unconstrained inversion is in good agreement with the shallow high resistivity volumes seen close to the well (Figure 3), and the inversion has also captured their relative lateral variations. The Bressay reservoir is seen in the well data as a thin but high resistivity anomaly at a depth of ~1.2 km (Figure 3), The unconstrained inversion is supposed to highlight only the large scale features in terms of depths to major stratigraphic boundaries, therefore, the result of the inversion will not resolve thinner resistors. It is intended to

DOI http://dx.doi.org/10.1190/segam2014-0534.1

find a slowly varying model that best fits the data.

The EM line of BK043 is crossing the Kraken heavy oil field (Figure 1). The reservoir is situated close to the top of the basement with a distance of separation less than ~150 m. The diffusive nature of EM field means that depth is often poorly constrained using CSEM data alone. In practice this is a typical situations that the EM inversion needs seismic structures to help to improve the depth resolution of the mapping. Here we see the unconstrained inversion has smoothed the resistivity contrast between the reservoir and the basement, whereas only a resistivity-thickness product was returned, means the high dimension features, such as the Kraken reservoir, will not be resolved in the final model.

The seismic guided inversion

Our proposed EM data integration workflow is aiming to facilitate an optimal procedure to combine the complementary information from the Towed EM and dual-sensor seismic data. The higher resolution of the seismic image makes it possible to determine the most appropriate locations of potential resistivity contrasts. We describe here the workflow how it incorporates information obtained from seismic data into an inversion of EM to improve the results of the unconstrained inversions presented above.

We setup line BK014 seismic guided inversion to have an isotropic 1Ωm half-space background, as shown in Figure 3. While the boundaries between the inter-bedded sands and shales in the overburden of Bressay were defined by the post-stack dual-sensor seismic data, the anisotropic resistivity variations within the layers above the top reservoir (indicated by the star) were accommodated by the lower and upper boundaries, i.e., the lowest and highest average resistivities, as constrained by the previous unconstrained anisotropic 2.5D inversions, whilst the remaining regions are all set as free parameter space for inversion. Note the seismic boundaries adopted here are free (not fixed) parameters, and been adopted only for the purpose of 'guiding' and to inform the EM inversion these geological interfaces mapped by seismic may be also be potential EM boundaries. Well logs provide a higher resolution measurement of the properties of a reservoir and the overburden strata at the location of the well. We upscale the log data using the arithmetic and harmonic average to approximate the vertical and horizontal resistivity with each layer. We tied the up-scaled log, 3/28A-6, vertical and horizontal resistivities, with the lowest and highest average resistivities, as constrained by the unconstrained anisotropic inversion, to estimate the lower and upper anisotropic resistivity inversion boundaries, respectively. However, in practice, we further extend the estimated inversion boundaries. We used the estimated smallest and the largest values between the horizontal and vertical boundaries in each layer to form only one set of the lower and upper boundaries for both vertical and horizontal resistivity inversions. In this way, we maximize the inversion-searching domain to ensure the use of the seismic and the unconstrained inversion results as a guide, which, at the mean time, provide the appropriate regularizations that the inversion requires.

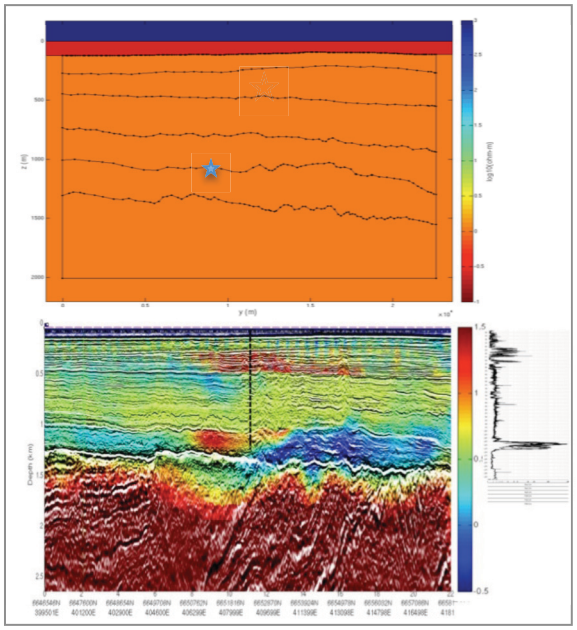

Figure 3 Top shows the seismic horizons adopted for guiding the inversion of line BK014, where the star indicates the seismically defined top reservoir interface. Bottom, seismic guided inversion results (vertical resistivities) for line BK014 (left), and well 3/28A-6 resistivity log (right). The thick black dotted line indicates the well location.

In Figure 3, the final result of the seismic guided inversion is shown. A prominent high resistivity anomaly is shown at the depth and lateral location of the known reservoir of Bressay. By comparing to the results obtained by the unconstrained inversion, as shown in Figure 2, both inversions consistently reveal a lateral extent of a large shallow resistive body in the overburden, in the depth range of ~500 – 800 m. The existence of high resistivity materials in the overburden is also evidenced by well-log data (Figure 3). The body seems due to a chimney-like intrusion where the seismic display the cross-cutting the primary reflections. The body might possibly be formed by gas leakage from the top of the reservoir (Figure 3). Compared to unconstrained inversion, the boundary between the overburden and the underlying formation constrained by the seismic guided inversion is much more consistent with the seismic image.

DOI http://dx.doi.org/10.1190/segam2014-0534.1

We conducted seismic guided inversion for line BK043 following similar procedures as the line BK014 inversion, described above. In addition, for this inversion, we have adopted a seismic horizon that define the top of the Heimdal sand as a 'cut' to break the Occam smooth regularization at the top of the reservoir (a sharp contrast in resistivity is allowed here). Figure 4 shows the final inversion retrieved model, indicating that the 'cut' is helpful to constrain the reservoir, but has no effect on other parts of the horizon where was 'cut' but the surface of body seismically defined sand (none resistive). The 'cut' also has little effect on the inversion for retrieving the background structure, as evidenced by comparing the two final models, obtained by the unconstrained (the top panel of Figure 2), to the seismic guided inversion (Figure 4).

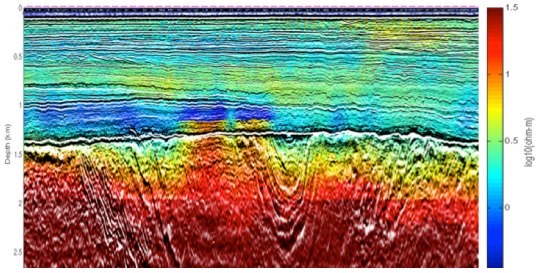

Figure 4 Same as Figure 2 but showing the seismic guided inversion result (vertical resistivities) for line BK043.

In Figure 4, the result of line BK043 seismic guided inversion result displays a localized strong EM anomaly corresponding to the main Heimdal sand body, as constrained by seismic, coincident with the location of the known Kraken reservoir. The inversion was able to vertically separate the reservoir from the below basement, while retrieving the basement boundary with lateral resistivity variations following more closely the amplitude of seismic reflections, as compared to the unconstrained inversions (Figure 2).

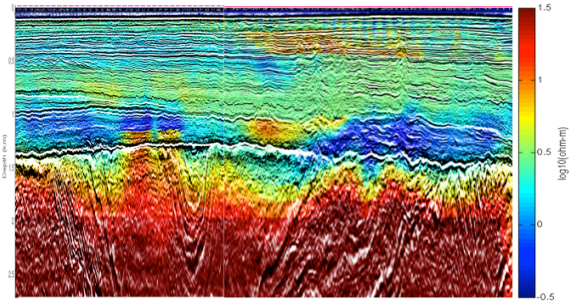

Figure 5 shows seismic guided inversion result (vertical resistivities) for the arbitrary line, obtained by stitching the two inversion results together from the line BK043 (Figure 4) and BK013 (Figure 3), as indicated in blue in Figure 1.

We investigate here further the lateral variation in resistivity in the overburden (depths between ~300 - 1000 m), as shown by the results from inversion of lines of BK014 and BK043. By focusing on the seismically constrained sub-surface structures of interest, we stitched the two sections together at the location where they cross to form an arbitrary line (see the line path footprint given by blue line in Figure 1). The resistivity profile for this newly formed arbitrary line, achieved simply by laying the two individual seismic guided inversion results side by side, is shown in Figure 5. What we observe here is a consistent seamless link of the two independently obtained models. The model displays an overall picture of the regional geology, however, it also reflects the structural complexities. In particular, it has highlighted the resistivity variations in the shallow structure and their close correlations with seismic variations (Figure 5).

From the above joint BBK towed streamer EM and seismic data analysis, we may summarize some of the BBK regional main structural features. There is a zone of higher resistivity in the shallow structure. One of the prominent features that anisotropic inversion shows (horizontal resistivities are not shown for brevity) is the existence of the overburden anisotropy at the same depth, while it recovers an isotropic resistive basement. Kerry et al. (2014) have studied in some detail the nature of the BBK anisotropy. Whereas anisotropic inversion clearly recovered these shallow anisotropic resistors in the overburden, isotropic inversion resulted in some strong artificial alternating stripes of resistive and conductive layers creating a final meaningless model that presented no plausible geological scenario. They have thus concluded that in the BBK region anisotropic inversion is mandatory.

Conclusions

We have presented a method of the seismic guided EM inversion, and it has been applied in the inversion of a towed streamer EM dataset acquired over a complex geological area of the BBK to illuminate the Bressay and Kraken heavy oil reservoirs. The data processing examples demonstrate the workflow can be used for exploring complex geological regions, and is applicable in a frontier exploration where CSEM and 3D seismic data co-exist.

Acknowledgements

The author would like to thank PGS for allowing the publication of this work, and to BlueGreen Geophysics for providing the MARE2DEM 2.5 D inversion code for data processing.

DOI http://dx.doi.org/10.1190/segam2014-0534.1

http://dx.doi.org/10.1190/segam2014-0534.1

EDITED REFERENCES

Note: This reference list is a copy-edited version of the reference list submitted by the author. Reference lists for the 2014 SEG Technical Program Expanded Abstracts have been copy edited so that references provided with the online metadata for each paper will achieve a high degree of linking to cited sources that appear on the Web.

REFERENCES

Constable, S. C., R. L. Parker, and C. G. Constable, 1987, Occam's inversion — A practical algorithm for generating smooth models from electromagnetic sounding data: Geophysics, **52**, 289–300, http://dx.doi.org/10.1190/1.1442303.

Karman, G. P., D. Ramirez, J. Voon, and L. M. Rosenquist, 2013, More than a decade of CSEM in Shell — Insights from a global look back: 2nd International CSEM Conference, Geological Society of Norway, Keynote Address.

Key, K., 2012, Marine EM inversion using unstructured grids: A 2D parallel adaptive finite element algorithm: 82nd Annual International Meeting, SEG, Expanded Abstracts, doi: 10.1190/segam2012-1294.1.

Key, K., Z. Du, J. Mattsson, A. McKay, and J. Midgley, 2014, Anisotropic inversion of towed EM data from Bentley, Bressay and Kraken using parallel adaptive finite elements: 76th Conference & Exhibition, EAGE, Extended Abstracts, 10.3997/2214-4609.20141250.

Morten, P., C. Twarz, V. Valente Ricoy-Paramo, and S. Sun, 2013, Improved resolution salt imaging from 3D CSEM anisotropic inversion: 75th Conference & Exhibition, EAGE, Extended Abstracts, Th 11 12.